Modification of Conductivity of P3HT by Addition of Endometallo Fullerene

Debmalya Roy, N. K. Tripathi, A. Saraiya, K. Ram

Nanoscience and Technology Division, DMSRDE, Kanpur 208013, India

Received 22 September 2008; accepted 22 March 2009
DOI 10.1002/app.30531
Published online 8 June 2009 in Wiley InterScience (www.interscience.wiley.com).

ABSTRACT: Germanium endometallo fullerene was synthesized by arcing Ge-impregnated graphite rod as anode and pure graphite rod as cathode. Photoluminescence (PL) and resistance measurements suggest that there are effective interactions at the interface of Ge endometallo fullerene and poly 3-hexyl thiophene (P3HT). Four-fold enhancement of conductance has been found by adding just one weight percentage of Ge endometallo fullerene in the P3HT matrix at room temperature. However, at lower and higher temperatures, the enhancement in conductivity is low compared with room temperature, indicating the efficient charge transfer across the interface at the temperature range of 300–350 K. Atomic force microscopy (AFM) images also confirm the fact that temperature makes the more ordered heterojunctions between P3HT and Ge endohedral metallofullerene, which, in turn, trigger charge separation across interfaces. A sharp quenching in PL intensity of P3HT at room temperature by adding Ge endometallo fullerene indicates a strong interaction between the two and this composite material can be useful in photovoltaic cell. © 2009 Wiley Periodicals, Inc. J Appl Polym Sci 114: 491–495, 2009

Key words: conducting polymer; endometallo fullerene; interfaces; resistance; photoluminescence

INTRODUCTION

The discovery of conducting polymer has opened up a plethora of applications in the field of electronics devices.[1–3] However, lack of solubilities of conducting polymers limit a wide range of applications.[4] Optimization of conductivity and solubility of a conducting polymer critically determines its fate for device fabrications. The conductivity of certain polymers can be raised to metallic level by chemical, electrochemical, or charge injection doping.[5,6] The mechanism of enhancement of conductivity by doping of an organic polymer is completely different from a classical inorganic semiconductor.[7] Doping in an inorganic semiconductor generates charge carriers that move in an electric field, this movement of charge is responsible for electrical conductivity in crystalline materials. In contrast, the doping of an organic polymer involves the partial oxidation or reduction of the polymer, each oxidation state then exhibits its own characteristic reduction potential.[8] On the other hand, electrons and holes can be trapped or injected into the π and π^* orbitals of a polymer and subsequently drastically alter the conductivity of the polymer.[9] The mobility of the charge carriers primarily depends on the orientation of the chains in polymer microstructure. Ordered orientation of polymer chains, thus, increases the mobility of excitons, which, in turn, enhances the conductivity of polymers.[10–12]

Because of very high surface to volume ratio of nanoparticles, the interfacial areas in the nanocomposite are large leading to more prominent effect of synergistic properties.[13,14] Photoinduced electron transfer is well established and utilized in heterojunction diodes using the composites of semiconducting polymer as donor and fullerene as acceptor.[15,16] The most efficient device architecture for polymeric photovoltaic is the bulk heterojunction as the possibility of exciton harvesting is maximum by creating a highly folded architecture such that all excitons are formed near a heterojunction.[17–19] P3HT is a conjugated polymer with good solubility, processability, and environmental stability.[20] The alkyl side chain length of regioregular polyalkyl thiophene affects the electrochemical and optical properties of conducting polymer.[21] With longer side chain length, their electrochemical band gaps are increased. Because of chromophore dilution, the absorption coefficient decreases by lengthening the side chain of polyalkyl thiophene. Because of the semicrystalline nature of its spin-cast films rr-P3HT shows the highest field-effect transistor mobilities for a conjugated polymer.[22] Ge endometallo fullerene shows fairly good amount of absorption in UV, visible, and NIR region, which leads to harvest more photons from sunlight and makes this material potentially more efficient for photovoltaic application.

Correspondence to: D. Roy (debmalya_roy@yahoo.com).

EXPERIMENTAL

Synthesis of endohedral Ge-doped fullerene was performed in electric arc reactor. GeO_2-impregnated 6-mm diameter graphite rod was used as anode, whereas pure graphite electrode of same diameter was used as cathode. The extraction of endohedral metallofullerene was performed by three-step solvent extraction using soxhlet under inert atmosphere at solvent boiling point. *O*-xylene was used first followed by *N*,*N* dimethylformamide. Freshly distilled aniline was then used to isolate metallofullerenes.[23] The various analytical techniques were used to characterize and evaluate the physical properties of Ge endometallo fullerene.

Energy dispersive X-ray (EDX) spectrum was recorded on a CARL ZIESS EVO 50 low-vacuum scanning electron microscope. The mass spectroscopic analysis was performed by a matrix-assisted laser desorption ionization (MALDI) technique using Bruker FLEX-PC2 ultraflex time of flight (TOF) mass spectrometer. Measurements were performed with α-cinnamic acid as the matrix using laser pulse of different wavelengths.

P3HT was purchased from Sigma–Aldrich Chemical and was used as received. For properties and characterization of P3HT, we follow the standard procedures.[24] Nanocomposite of P3HT and Ge endometallo fullerene was assembled from chlorobenzene with desired weight percentage of 1 to 10. The mixture was kept overnight at 75°C and a stream of N_2 was flown over the sample to evaporate the organic solvent. The nanocomposite was finally mixed thoroughly using a ball-milling machine at 200 rpm for 30 min.

Comparative resistivity was studied on the pallets made out of P3HT and P3HT with one weight percentage of Ge endometallo fullerene. Resistance measurements at different temperatures of the samples were performed using four-probe low-temperature-resistance measurements in the temperature range of 500–10 K. Keithley's current source model-220 and a nano-voltmeter model-2182 were used to record the resistance at different temperatures. The samples were cooled down by a closed-cycle refrigerator (CTI Cryogenics make). The ohmic contacts were made by silver paste.

Comparative PL of the thin films of P3HT and different weight percentages of Ge endometallo fullerene were recorded at $\lambda_{ex} = 480$ nm. Thin films for PL measurement were prepared by drop casting of samples homogeneously dispersed in acetone on quartz plates.

AFM images were recorded on an AFM Nanoscope II (Digital Instruments, USA). P3HT and Ge endohedral metallofullerene were dissolved in chlorobenzene at 100 : 1 weight ratios and thin films were spin casted on silicon wafer using a high-speed spin coater. Thin film on Silicon wafer was annealed in vacuum for 30 min at required temperatures and then the images of the surface were taken by AFM.

RESULTS AND DISCUSSION

EDX analysis of the aniline extract shows the characteristic peak for Ge, indicating the presence of germanium in the fullerene cage (Fig. 1). UV spectrum of Ge-encapsulated fullerene shows a similar pattern like the other endohedral metallofullerenes. Normally, the absorption spectra of metallofullerenes have long tails to the red region, which is also seen in Ge-encapsulated fullerene. Fourier transform infrared spectrum below 400 cm^{-1} using CsI crystal does not show any metal–carbon signal, this also indicates that Ge metal is caught inside the fullerene cage. Abundance of $Ge@C_{82}$ in the product is confirmed by the presence of an intense peak around 1058 m/z in MALDI–TOF spectrum (Fig. 2) of aniline extract. Because of aerobic condition of the extraction procedure, the abundance of $Ge@C_{60}$ is low in the final product. The presence of aniline in the aniline extract could be attributed to the formation of aniline adduct with fullerene and metallofullerene during refluxing with aniline. The peaks at 813, 887, and 1151 m/z indicate the formation of monoaniline adduct with C_{60}, $Ge@C_{60}$, and $Ge@C_{82}$.

Sharp quenching in the PL intensities (Fig. 3) by addition of different weight percentages of Ge endometallo fullerene indicates strong interactions between the polymer matrix and the filler material. At higher weight percentage loading of Ge endometallo fullerene, the photons harvesting have been driven by metallofullerene and hence radiative recombination of electron–hole pairs dominate. However, at lower weight percentage, addition of metallofullerene a strong interaction is evident

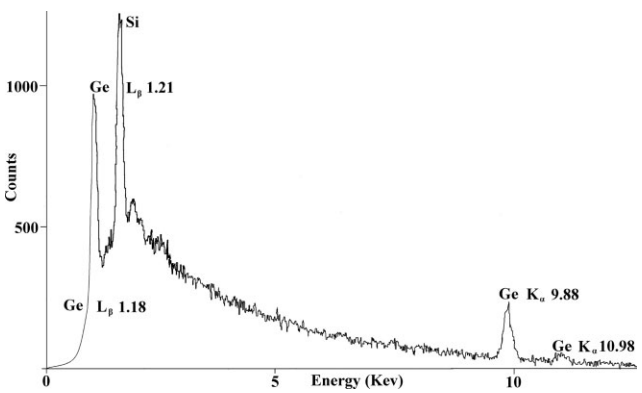

Figure 1 Energy dispersive X-ray spectrum of the aniline extract of Ge endometallo fullerene film on Si substrate grown by drop casting of aniline extract.

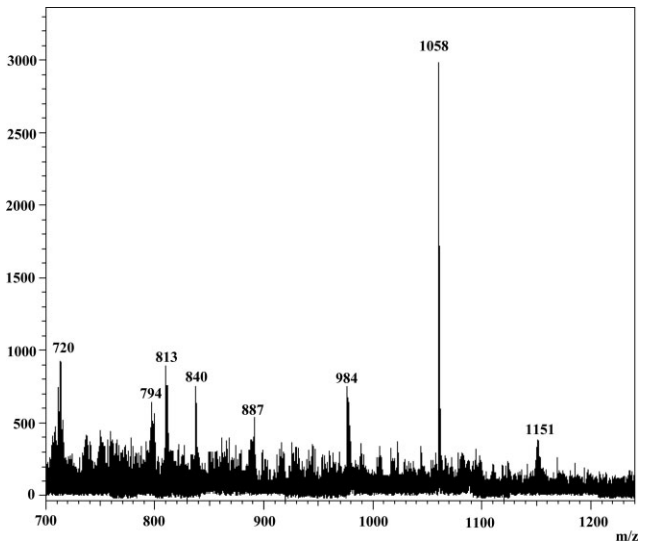

Figure 2 Matrix-assisted laser desorption ionization-time of flight mass (MALDI–TOF) spectrum of aniline extract of Ge endohedral metallofullerene.

between the Ge endometallo fullerene and P3HT matrix, which leads to separation of electron–hole pairs at the interface, leading to quenching of PL intensity.

Conductance measurements of the pallets made out of P3HT and P3HT with one weight percentage of Ge endometallo fullerene were performed by four-probe low-temperature-resistance measurements in the temperature range of 500–10 K. Comparative conductance measurement plot (Fig. 4) shows the enhancement of conductance of P3HT by addition of one weight percentage of Ge endometallo fullerene. This phenomenon clearly indicates the charge transfer across the interface. Ge endometallo fullerene makes the P3HT matrix more ordered, resulting in the enhancement of electron and hole mobilities in the matrix.[25]

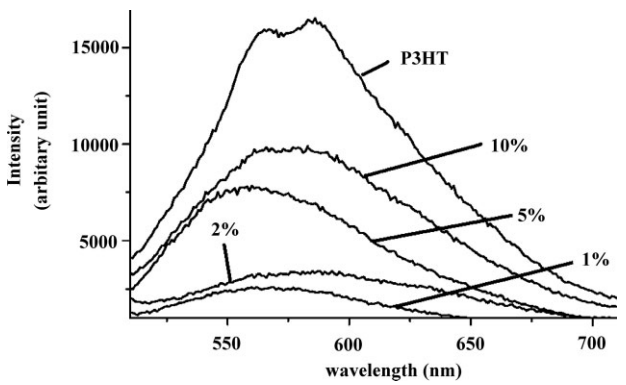

Figure 3 Comparative PL intensities of P3HT and different weight percentages of Ge endometallo fullerene at λex = 480 nm.

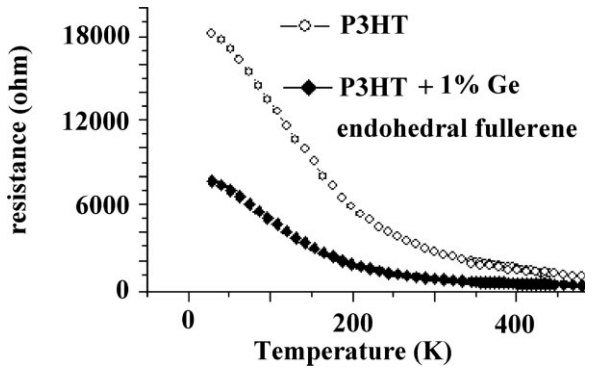

Figure 4 Comparative resistances of the pallets made out of P3HT and P3HT with one weight percentage of Ge endometallo fullerene.

The temperature-dependent resistances of P3HT and P3HT–Ge endometallo fullerene nanocomposite show semiconducting type behavior, indicating the higher availability of charge carriers at high temperature. However, it is evident from Figure 5 that the difference of resistances of P3HT and P3HT–Ge endometallo fullerene nanocomposite is highest at the temperature range of 300–350 K. At lower and higher temperatures, the differences in resistances are not that significant in P3HT–Ge endometallo fullerene nanocomposite. Similar temperature-dependent conductivity has also been seen in polyaniline fibers.[26] At low temperature, crystallinity of the composite polymer matrix is low and increasing the temperature helps to align P3HT in nanocomposite due to lattice vibration of the matrix, resulting in higher conductivity.

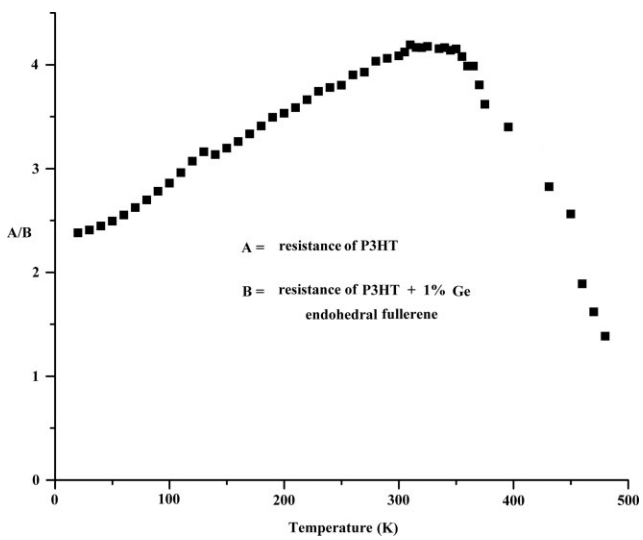

Figure 5 The difference in resistances of P3HT and P3HT–Ge endometallo fullerene nanocomposite (weight percentage ratio 100 : 1) from 10 to 500 K.

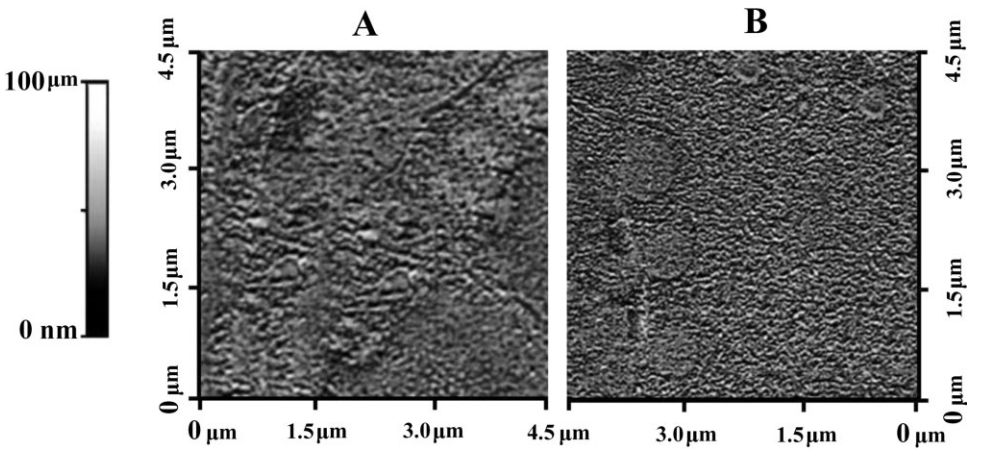

Figure 6 (A) AFM images of P3HT and one weight percentages of Ge endometallo fullerene at 20°C and (B) AFM images of P3HT and one weight percentages of Ge endometallo fullerene at 50°C.

AFM images (Fig. 6) of P3HT and one weight percentage Ge endohedral metallofullerene at 20°C and 50°C clearly confirms the facts that temperature makes the more ordered heterojunctions between P3HT and Ge endohedral metallofullerene, which, in turn, trigger charge separation across interfaces. However, after a limiting temperature (~ 350 K in this case; Fig. 5), the alignment of P3HT is started degrading due to very high thermal energy assisted phonon coupling in the nanocomposite matrix. At very high temperature (~ 500 K in this case; Fig. 5), the resistance ratio of polymer and the composite is almost one, indicating the complete disruption of alignment in polymer–filler network. Therefore, only in a certain temperature range where the alignment of polymer chains in the nanocomposite matrix (P3HT-Ge endometallo fullerene) is best, we can see an efficient charge transfer at the interface.

CONCLUSION

Our study is aimed to focus the importance of temperature for the alignment of polymer chains in the nanocomposite matrix. The efficient charge transfer across the interface is only evident in certain temperature range where crystallinity of polymer–filler network is the maximum. Using the intensities of PL and resistance measurements of Ge endometallo fullerene and P3HT, we showed an effective interaction at the interface. AFM images and comparative resistance measurement show that the most efficient charge transfer in the endometallo fullerene and P3HT matrix happens at the temperature range of 300–350 K. Semiconducting type behavior indicates the lower availability of charge carriers at low temperature range. The higher temperature destroys the ordered nanocomposite morphology due to phonon coupling of polymer matrix. Temperature, therefore, is the key for efficient charge transfer across the interface.

The authors are grateful to the Director, DMSRDE, Kanpur for the permission to publish this manuscript. We are thankful to Dr. Kingsuk Mukhopadhyay for his constant help and support. We also thank Prof. A. Pradhan, IIT, Kanpur for permitting us to record photoluminescence (PL) in her laboratory and acknowledge the help of Prof. Vikram Kumar, NPL for recording AFM images.

References

1. Gospodinova, N.; Terlemezyan, L. Prog Polym Sci 1998, 23, 1443.
2. Groenendaal, L.; Jonas, F.; Freitag, D.; Pielartzik, H.; Reynolds, J. R. Adv Mater 2000, 12, 481.
3. Kuhn, H. H.; Child, A. D.; Kimbrell, W. C. Synth Met 1995, 71, 2139.
4. Bhattacharya, A.; De, A. Prog Solid State Chem 1996, 24, 141.
5. Chiang, C. K.; Gau, S. C.; Fincher, C. R.; Park, Y. W.; Macdiarmid, A. G.; Heeger, A. J Appl Phys Lett 1978, 33, 18.
6. Salaneck, W. R.; Lundstrom, I.; Haung, W. S.; Macdiarmid, A. G. Synth Met 1986, 13, 291.
7. Roth, S. One-Dimensional Metals; VCH: Weinheim, 1995.
8. Nigrey, P. J.; Macdiarmid, A. G.; Heeger, A. J. Chem Commun 1979, 96, 594.
9. Yu, G.; Gao, J.; Hummelen, J. C.; Wudl, F.; Heeger, A. J. Science 1995, 270, 1789.
10. Heeger, A. J. Synth Met 2001, 125, 23.
11. Roy, D.; Basu, P. K.; Raghunathan, P.; Eswaran, S. V. J Appl Polym Sci 2004, 91, 2096.
12. Kaiser, A. B. Adv Mater 2001, 13, 927.
13. Thostenson, E. T.; Li, C.; Chou, T. W. Compos Sci Technol 2005, 65, 491.
14. Harris, P. J. F. Int Mater Rev 2004, 49, 31.
15. Yoo, S.; Domercq, B.; Kippelen, B. J. Appl Phys 2005, 97, 103706.
16. Günes, S.; Neugebauer, H.; Sariciftci, N. S. Chem Rev 2007, 107, 1324.
17. Bundgaard, E.; Krebs, F. C. Sol Energ Mater Sol Cells 2007, 91, 954.

18. Mihailetchi, V. D.; Xie, H.; Boer, B.; Popescu, L. M.; Hummelen, J. C.; Blom, P. W. M.; Koster, L. J. A. Appl Phys Lett 2006, 89, 012107.
19. Brabec, C. J.; Sariciftci, N. S.; Hummelen, J. C. Adv Funct Mater 2001, 11, 15.
20. Ibrahim, M. A.; Rotha, H. K.; Zhokhavetsb, U.; Gobschb, G.; Sensfuss, S. Sol Energ Mater Sol Cells 2005, 85, 13.
21. Ibrahim, M. A.; Rotha, H. K.; Schroedner, M.; Kalvin, A.; Zhokhavets, U.; Gobsch, G.; Scharff, P.; Sensfuss, S. Org Electron 2005, 6, 65.
22. Sirringhaus, H.; Brown, J.; Friend, R. H.; Nielsen, M. M.; Bechgaard, B. M. W.; Spiering, A. J. H.; Janssen, R. A. J.; Meijer, E. W.; Herwig, P.; Leeuw, D. M. de Nat 1999, 401, 685.
23. Roy, D.; Tripathi, N. K.; Ram, K.; Sathymurthi, N. Communicated.
24. Mccullough, R. D. Adv Mater 1999, 10, 93.
25. Yanga, C. Y.; Caoa, Y.; Smithb, P.; Heeger, A. J. Synth Met 1993, 53, 293.
26. Adams, P. N.; Pomfret, S. J.; Monkman, A. P. Synth Met 1999, 101, 685.